



Photocatalytic degradation of reactive brilliant red X-3B over BiOI under visible light irradiation

Lingyun Zhou^{a,*}, Wei Guo^b, Guohong Xie^a, Jinglan Feng^c

^aDepartment of Environmental Science, College of Resource and Environment, Henan Institute of Science and Technology, East of HuaLan Road, Xinxiang, Henan 453003, China

Tel. +86 373 3040147; email: lyzhou1980@163.com

^bDepartment of Chemistry, Xinxiang Medical University, East of JinSui Road, Xinxiang, Henan 453003, China

^cKey Laboratory for Yellow River and Huaihe River Water Environmental and Pollution Control Ministry of Education, Henan Key Laboratory for Environmental Pollution Control, Henan Normal University, Xinxiang, Henan 453007, China

Received 25 September 2012; Accepted 9 January 2013

ABSTRACT

In this work, bismuth oxyiodide (BiOI) photocatalyst which is capable of responding to visible light was prepared and characterized by X-ray diffraction (XRD), Scanning electron microscopy (SEM), Transmission electron microscopy (TEM), and UV–vis diffuse reflectance spectroscopy (UV–vis DRS). Photocatalytic activity of this material was evaluated by using reactive brilliant red X-3B as a representative dye wastewater. It was found that BiOI had a strong visible light absorption, and the band gap energy was estimated to be 1.76 eV. This material exhibited good photocatalytic activity under visible light irradiation. For example, the removal efficiency of reactive brilliant red X-3B by BiOI was as high as 95% within 2-h visible light irradiation under the specific conditions: initial reactive brilliant red X-3B concentration of 10 mg L⁻¹, catalyst dosage of 2.0 g L⁻¹, and initial solution pH of 7. The photocatalytic degradation of reactive brilliant red X-3B by BiOI under visible light irradiation was found to follow the pseudo-second-order reaction. The results of the recycled experiments indicated that the photocatalytic activity kept stable in the photocatalysis. Furthermore, it was found that the degradation of methyl orange (MO) was also effective under visible light irradiation. From the viewpoint of energy efficiency and conservation, BiOI is an efficient visible light-responsive photocatalyst for the degradation of azo dye wastewaters.

Keywords: BiOI; Visible light; Dye wastewater; Photocatalyst; Kinetics

1. Introduction

Reactive dyes are widely used in textile industry in the recent years owing to their superior performance, but they are environmentally hazardous and difficult to treat effectively by classical methods

because the textile wastewater is resistant to the conventional biological treatment due to their stability and toxicity. To resolve this problem, several methods such as adsorption [1], nanofiltration [2], ozonation [3], electrochemical [4], etc. were used to remove the dyes from wastewater. In the meantime, photocatalysis for the purification of the dye-containing

*Corresponding author.

wastewater is attracting more and more attention as it is cost-effective [5–7], and has been investigated as an alternative to conventional methods. From the viewpoint of energy efficiency and conservation, the development of efficient visible light-induced photocatalysts for the degradation of reactive dyes is one of the most important issues in the field of photocatalysis.

Bismuth oxyhalides have been demonstrated excellent photocatalytic activities as promising photocatalysts recently [8–14]. Among them, bismuth oxyiodide (BiOI) has the smallest band gap and strong absorption in visible light region, thus it might have an excellent photocatalytic performance under sunlight irradiation [15]. Herein, we synthesized BiOI composite by a template-free method at room temperature and investigated the photocatalytic performance of reactive brilliant red X-3B over BiOI under visible light irradiation, hoping to get some useful parameters to direct practical application.

In this work, photocatalyst BiOI was synthesized and characterized by X-ray diffraction (XRD), Scanning electron microscopy (SEM), Transmission electron microscopy (TEM), and UV–vis diffuse reflectance spectra (UV–vis DRS). Its degradation efficiency was evaluated by using reactive brilliant red X-3B as a representative reactive dye wastewater in detail; various experimental parameters such as the initial concentration of reactive brilliant red X-3B, initial solution pH, and catalyst dosage were optimized systematically and the reaction dynamic model was studied. In order to further evaluate the photocatalytic properties of BiOI, the photocatalytic degradation efficiency of methyl orange (MO) was also determined under visible light irradiation. It was demonstrated that BiOI exhibited an excellent visible light photocatalytic activity for the degradation of the reactive brilliant red X-3B and MO.

2. Materials and methods

2.1. BiOI photocatalyst preparation and characterization

The BiOI powders were synthesized by a soft chemical method similar to Ref. [16]. In brief, Bi (NO_3)₃·5H₂O (AR, 99.0%) powders were slowly added into an aqueous solution containing stoichiometric amounts of KI (AR, 98.5%), then the mixtures were adjusted to pH 3 by using diluted HNO₃ solution and stirred vigorously for 20 h. After the reaction was complete, the resulting solid products BiOI were collected by filtration, then washed several times with deionized water, and dried at 80 °C in a vacuum oven before further characterizations and photocatalytic

activity evaluations. All the reagents were purchased from Sinopharm Chemical Reagent Co. (Shanghai, China) and used without further purifications.

The crystallinity of the as-prepared sample was characterized by powder XRD on a Bruker D8-Advance (Germany) equipped with a rotating anode with Cu K α radiation in the range of 10–80° while the voltage and electric current were held at 40 kV and 40 mA, respectively. SEM images were obtained on a JSM-63,901 field emission scanning electron microscope (Japan). TEM images were obtained on a JEM-100SX electron microscope (Japan) at an accelerating voltage of 80 kV. UV–vis DRS was measured at room temperature on a Hitachi U-3010 spectrophotometer by using BaSO₄ as reference. Zeta potential (mV) of BiOI at different pH values was measured by a nano-ZS90 zetasizer (England). The total organic carbon (TOC) was measured by a Shimadzu 5000A-TOC analyzer (Japan).

2.2. Photocatalytic reactions

Photocatalytic activity of BiOI samples was evaluated by the degradation of reactive brilliant red X-3B and MO in water under visible light irradiation. Photocatalytic reactor (Fig. 1) consists of three parts, a quartz cell with a circulating water jack, a 500 W

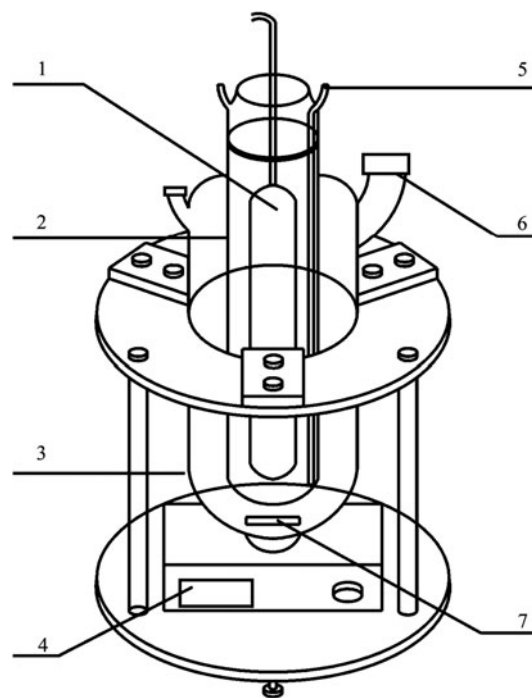


Fig. 1. Photocatalytic reaction device diagram: 1-xenon long-arc lamp, 2-quartz cell, 3-reaction cell, 4-indicator, 5-cooling water inlet, 6-sample connection, and 7-magnetic stirrer.

xenon long-arc lamp placed inside the quartz cell, and a hardened glass reactor with a magnetic stirring instrument in the bottom to keep the solution uniform. In all experiments, the reaction temperature was kept at room temperature to prevent any thermal catalytic effect by the circulating water jack. The volume of initial reactive brilliant red X-3B solution, with the concentration of 20 mg L^{-1} , is 250 mL. The powder concentration in the reactive brilliant red X-3B aqueous solution ranges from 0.5 to 4.0 g L^{-1} . Visible light illumination was conducted after the suspension was strongly magnetically stirred in the dark for 30 min to reach the adsorption–desorption equilibrium of reactive brilliant red X-3B or MO on catalyst surfaces. During irradiation, about 5 mL suspension was continually taken from the reaction cell at given time intervals for subsequent reactive brilliant red X-3B concentration analyzed by UV–vis spectrophotometer (TU-1901 PGENERAL China) after filtering.

The photocatalytic degradation efficiency (η) could be calculated as the following equation.

$$\eta = \left(1 - \frac{C_t}{C_0}\right) \times 100\% \quad (1)$$

where C_0 and C_t are the concentration of reactive brilliant red X-3B or MO at $t=0$ and $t=t$, respectively.

3. Results and discussion

3.1. BiOI photocatalyst Characterization

As the X-ray diffraction pattern shown in Fig. 2, the sample BiOI was well crystallized, and no distinct impurities signals were observed. All of the diffraction peaks could be well indexed to JCPDS File No. 73–2062.

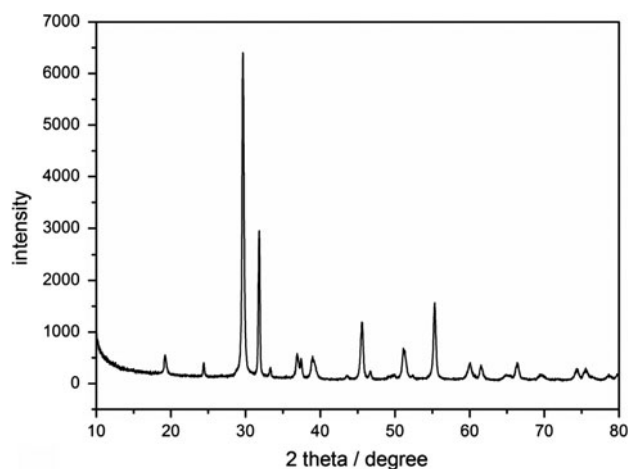


Fig. 2. The XRD pattern of BiOI.

The grain size, morphology, and structure of BiOI are shown in Fig. 3. It can be seen from Fig. 3(a), the morphology of BiOI is dominated by plate particle sizes from 400 to 600 nm and the thickness of the plates is about 50 nm. Actually, this is determined by its intrinsic layer structure [17], which can be seen from Fig. 3(b). The layered structure is considered to be favor of electronic transmission between the layers. This contributes to charge separation so that excited photo-formed electron and hole pairs can reduce and oxidize chemical substances, which consequently would help to enhance the photocatalytic activity of the photocatalyst.

UV–vis DRS of the BiOI powders are shown in Fig. 4(a). Clearly, BiOI powders have obvious absorption edges in the visible light region (400–650 nm).

The optical absorption of BiOI powders near the band edge obeys the following formula [18]

$$\alpha h\nu = A(h\nu - E_g)^{n/2} \quad (2)$$

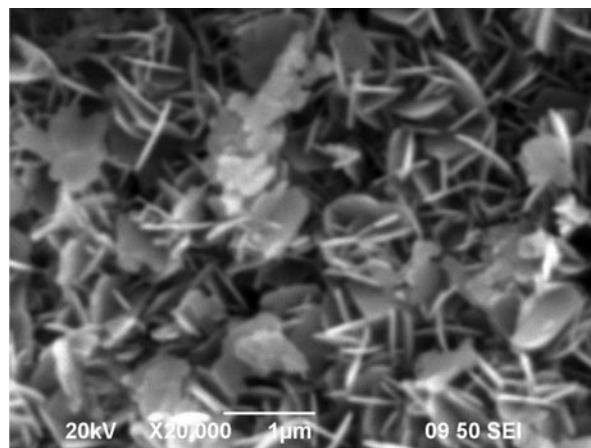


Fig. 3(a). The SEM image of BiOI.

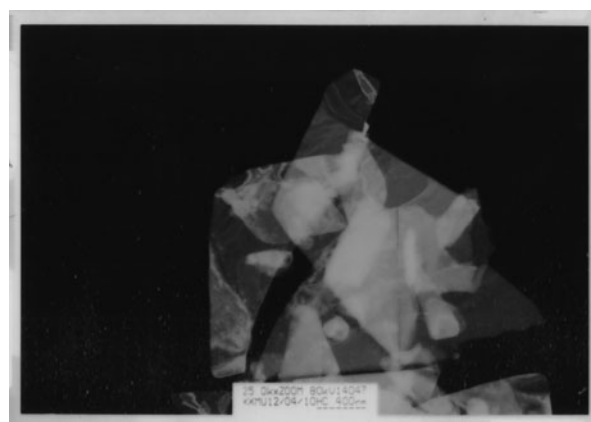


Fig. 3(b). The TEM image of BiOI.

in where α , ν , A , and E_g are absorption coefficient, light frequency, proportionality constant, and band gap energies, respectively. In Eq. (2), n decides the characteristics of the transition in a semiconductor; in other words, a direct transition for $n=1$ and an indirect transition for $n=4$. The E_g values of BiOI can be determined from a plot of $(\alpha h\nu)^{1/2}$ vs. photon energy ($h\nu$) which is shown in Fig. 4(b). The estimated band gap energies for BiOI was about 1.76 eV, which is close to the values reported in the literatures [15,18] and is smaller than the band gap of TiO₂ P25 (about 3.2 eV).

3.2. Photocatalytic degradation experiments of brilliant red X-3B

3.2.1. Photocatalytic degradation of reactive brilliant red X-3B

BiOI exhibited a high photocatalytic activity to remove reactive brilliant red X-3B (initial concentra-

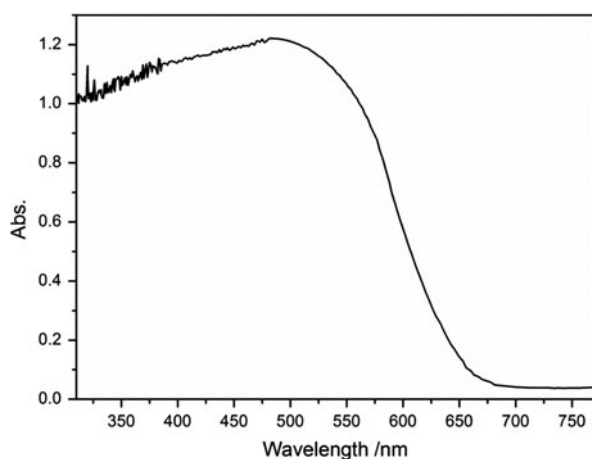


Fig. 4(a). UV-vis absorption spectrum of BiOI.

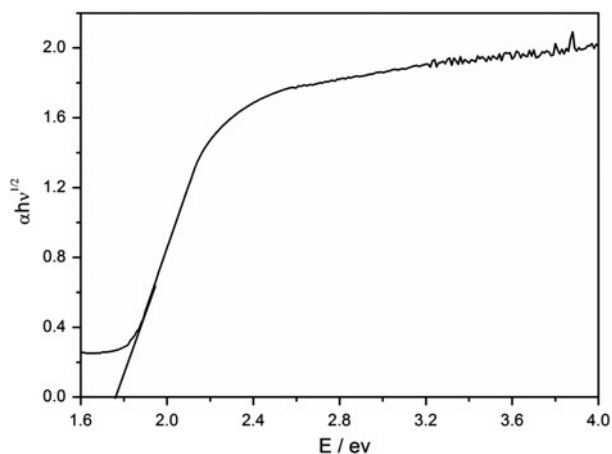


Fig. 4(b). Plots of $(\alpha h\nu)^{1/2}$ vs. photon energy ($h\nu$) for BiOI.

tion of 20 mg L⁻¹) under visible light irradiation (Fig. 5(a)). After 120 min of photocatalysis, the degradation efficiency over BiOI reached to 75%, while the degradation efficiency over TiO₂ P25 was only 26%. It suggested that the as-prepared BiOI showed much higher photoactivities for reactive brilliant red X-3B degradation than that of TiO₂ P25. At the meantime, it was found that the photolysis by Xenon lamp irradiation and adsorption on BiOI under dark condition was unapparent and could almost be neglected. The UV-vis spectral variations taking place during the photocatalysis over BiOI is given in Fig. 5(b). And, the

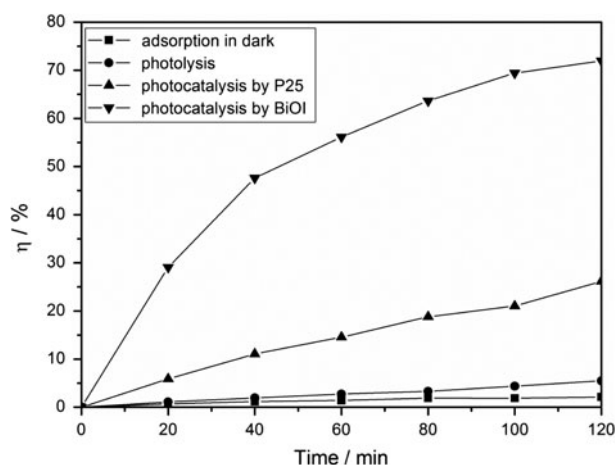


Fig. 5(a). Photocatalytic efficiency of reactive brilliant red X-3B at 20 mg L⁻¹ of initial reactive brilliant red X-3B concentration, 2.0 g L⁻¹ of catalyst dosage, and initial pH 7.

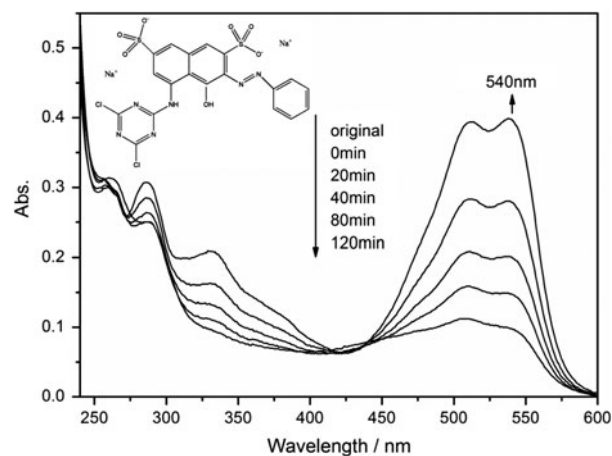


Fig. 5(b). UV-vis spectra evolution of reactive brilliant red X-3B during the photocatalytic reaction at 20 mg L⁻¹ initial reactive brilliant red X-3B concentration, 2.0 g L⁻¹ catalyst dosage, and initial pH 7 (the molecular structure of reactive brilliant red X-3B inserted).

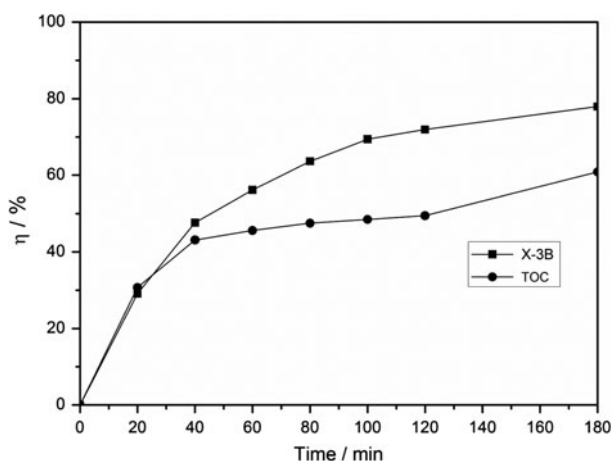


Fig. 5(c). Temporal change in reactive brilliant red X-3B and TOC removal during the photocatalytic reaction at 20 mg L^{-1} initial reactive brilliant red X-3B concentration, 2.0 g L^{-1} catalyst dosage, and initial pH 7.

molecular structure of reactive brilliant red X-3B is also included. From Fig. 5(b), the reactive brilliant red X-3B aqueous solution shows three major absorption peaks at 286, 332, and 540 nm, which are attributed to the benzene ring, naphthalene ring, and azo bond ($-\text{N}=\text{N}-$), respectively. The specific peaks become smoother gradually during the degradation processes, which indicated that the catalyst not only destroyed the chromophore of reactive brilliant red X-3B but also decomposed the benzene ring and naphthalene ring partly. Additionally, 40.6% of TOC was removed from the reaction system (the initial concentration of X-3B was 20 mg L^{-1} , pH was 7) after 60-min reaction with BiOI under visible light irradiation while 60.9% was removed in 180 min (Fig. 5(c)), suggesting that part of the reactive brilliant red X-3B was mineralized after 180-min visible light irradiation.

3.2.2. Effect of solution pH

The effect of pH on the degradation of reactive brilliant red X-3B was investigated by keeping all other experimental conditions constant and varying the initial pH of the reactive brilliant red X-3B solution from 3 to 11. The experimental results (Fig. 6) reveal that photodegradation efficiency under neutral and acid conditions is significantly higher than that under alkaline condition. The pH-dependent photodecomposition can be mainly attributed to the variation of surface charge properties of the photocatalyst at different pH values, which consequently changes the absorption behavior of a dye on a catalyst surface. Zeta potential (mV) of BiOI determined are: pH 3,

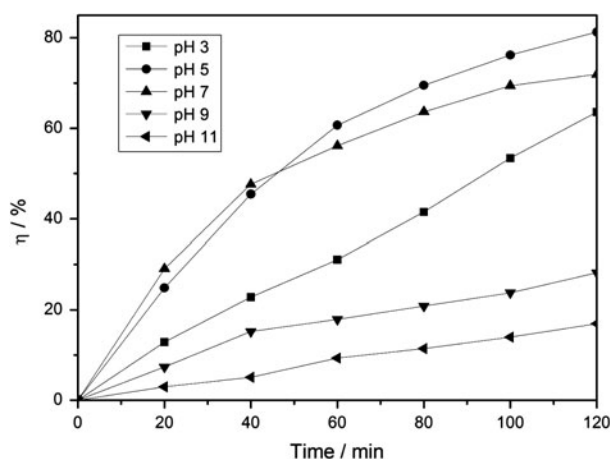


Fig. 6. Effect of solution pH on the photocatalytic degradation efficiency of reactive brilliant red X-3B at 20 mg L^{-1} of initial reactive brilliant red X-3B concentration and 2.0 g L^{-1} of catalyst dosage.

–29.1; pH 5, –32.1; pH 7, –32.4; pH 9, –35.5; pH 11, –52.3 eV, respectively. Lower potential values equate to more negative charges on a catalyst surface. Reactive brilliant red X-3B is an anionic dye. Thus, in the alkaline (pH 9 and 11) solution, the electrostatic repulsion between the catalyst surface and dye molecules is higher than that in the acidic solution, resulting in the reduction of reactive brilliant red X-3B adsorption on the catalyst surface, and in turn, the decrease of the removal efficiency of reactive brilliant red X-3B. But, the degradation efficiency at the lowest pH value (pH 3) is worse than that at pH 5, we deduced that it is probable because it is disadvantageous to the production of hydroxyl radicals on the BiOI surface. It is noted that both the lower and higher pH values are not propitious for the degradation of dyes on the catalyst and the degradation efficiency was higher for the pH value in the range of 5–7. As the pH range is close to the pH range of natural water, the BiOI photocatalyst could be used in wastewater systems directly without adjusting pH, resulting in the reduction for the costs of wastewater disposals.

3.2.3. Effect of catalyst dosage

Experiments were performed to study the variations in the rate of degradation at different catalyst dosage ranging from 0.5 to 4.0 g L^{-1} . It is observed from Fig. 7 that the degradation efficiency increases sharply with the catalyst concentration up to 4.0 g L^{-1} . This is probably due to an increased number of available adsorption and catalytic sites on the surface of BiOI catalyst. Because a further increase in catalyst

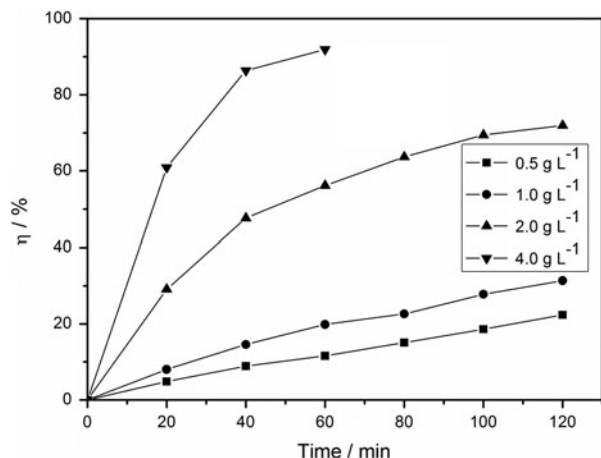


Fig. 7. Effect of catalyst dosage on the photocatalytic degradation efficiency of reactive brilliant red X-3B at 20 mg L^{-1} initial reactive brilliant red X-3B concentration and initial pH 7.

concentration may cause light scattering and screening effect and thus reduce the specific activity of the catalyst [19], the optimum catalyst dosage of BiOI for degradation is 4.0 g L^{-1} .

3.2.4. Effect of initial reactive brilliant red X-3B concentration and the relevant degradation kinetics

The effect of reactive brilliant red X-3B concentration on degradation efficiency was investigated by varying the concentration from 10 to 40 mg L^{-1} under 180-min irradiation with a fixed pH (pH=7) and catalyst dosage (2.0 g L^{-1}). The results are depicted in Fig. 8(a). It is clear that the degradation efficiency decreases with the increasing concentration of reactive

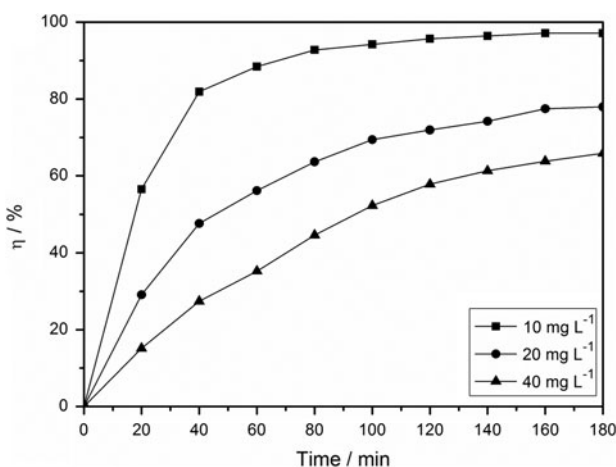


Fig. 8(a). Effect of initial concentrations of reactive brilliant red X-3B on the photocatalytic degradation efficiency at 2.0 g L^{-1} catalyst dosage and initial pH 7.

brilliant red X-3B from 10 to 40 mg L^{-1} . The pseudo-first-order kinetic equation and pseudo-second-order kinetic equation were, respectively, used to explore the photocatalytic degradation of reactive brilliant red X-3B.

On the basis of the chemical reaction kinetics theory, the pseudo-first-order kinetics can be expressed as

$$-dC/dt = kC \quad (3)$$

Integration of the above equation will lead to the following expected relation:

$$\ln(C_t/C_0) = -kt \quad (4)$$

where k and t are the apparent reaction rate constant and time, respectively. C_t and C_0 are the reactant concentration at time $t=t$ and $t=0$. According to Eq. (4), the plot of $\ln(C_t/C_0)$ vs. t is shown in Fig. 8(b). It can be seen that the curves were almost linear at the initial stage for the reactive brilliant red X-3B solutions with different concentration. However, with the increasing of reaction time, the slopes tended to decrease and the curves began to depart from the straight line.

In this study, the absorbing efficiency of light energy by BiOI was very high at the beginning of the reaction. The excited photo-formed electron and hole pairs were so sufficient that the collision frequency of reactive brilliant red X-3B molecules with e^- and h^+ depended mainly on the dye concentration. With the reaction going on, excited e^- and h^+ in the system decreased gradually, thus the collision frequency of reactive brilliant red X-3B molecules with excited e^-

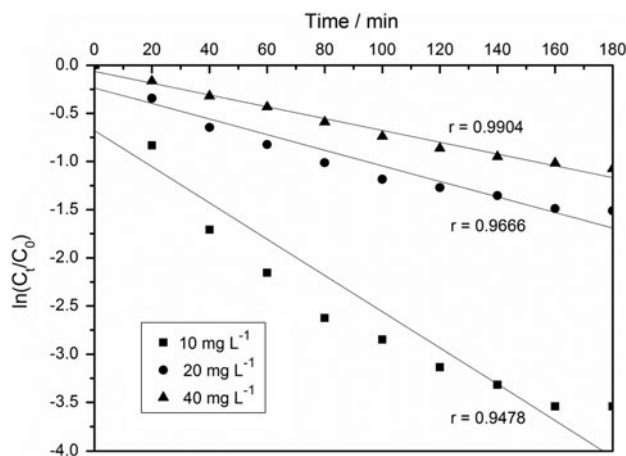


Fig. 8(b). Pseudo-first-order linear plots of $\ln(C_t/C_0)$ vs. irradiation time for the degradation kinetics at 2.0 g L^{-1} catalyst dosage and initial pH 7.

and h^+ began to depend on the quantity of excited e^- and h^+ . Pseudo-first-order kinetic equation was met if the rate of the reaction was controlled only by the dye concentration while having nothing to do with the other reactants. So, the whole process of the visible light-induced photocatalytic of reactive brilliant red X-3B over BiOI could not be well fitted using pseudo-first-order kinetic equation.

On the basis of the chemical reaction kinetics theory, the pseudo-second-order kinetics can be expressed as

$$-dC/dt = kC^2 \quad (5)$$

Integration of the above equation will lead to the following expected relation:

$$1/C_t = kt + 1/C_0 \quad (6)$$

where k and t are the apparent reaction rate constant and time, respectively. C_t and C_0 are the reactant concentration at time $t=t$ and $t=0$. According to Eq. (6), a plot of $1/C_t$ vs. t will yield a slope (k). The results are displayed in Fig. 8(b). The linearity of the plot suggests that the photodegradation reaction approximately obeys the pseudo-second-order kinetics (Related coefficient >0.96); with (k) as $2.70E-4$, $9.18E-4$, and $7.25E-3 \text{ min}^{-1}$ in the reactive brilliant red X-3B concentration of 10, 20, and 40 mg L^{-1} , respectively. The apparent reaction rate constant decreased with an increase in the concentration of reactive brilliant red X-3B. The presumed reason is that a mass of visible light may be absorbed by the reactive brilliant red X-3B molecules in aqueous solution rather than the catalyst particles for high reactive brilliant red X-3B concentration, which can reduce the efficiency of the catalytic reaction. Another possible reason is that the intermediate products formed upon photocatalytic degradation of reactive brilliant red X-3B may compete with the reactive brilliant red X-3B molecules for the limited adsorption and catalytic sites on the surface of catalyst particles, and thus inhibit the degradation of reactive brilliant red X-3B to a certain extent (Fig. 8(c)).

3.2.5. Recyclability of the photocatalyst

The photocatalytic stability of the BiOI catalyst was also evaluated by recycled experiments. After every 120 min of photodegradation, the separated photocatalysts were washed with deionized water and dried. The decrease of reactive brilliant red X-3B in every run is shown in Fig. 9(a). After three recycled

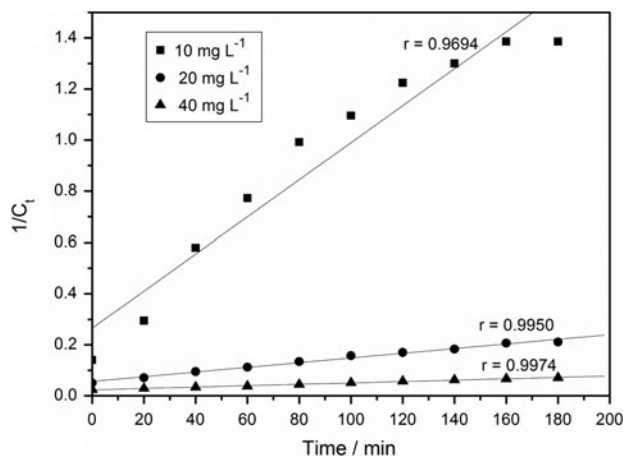


Fig. 8(c). Pseudo-second-order linear plots of $1/C_t$ vs. irradiation time for the degradation kinetics at 2.0 g L^{-1} catalyst dosage and initial pH 7.

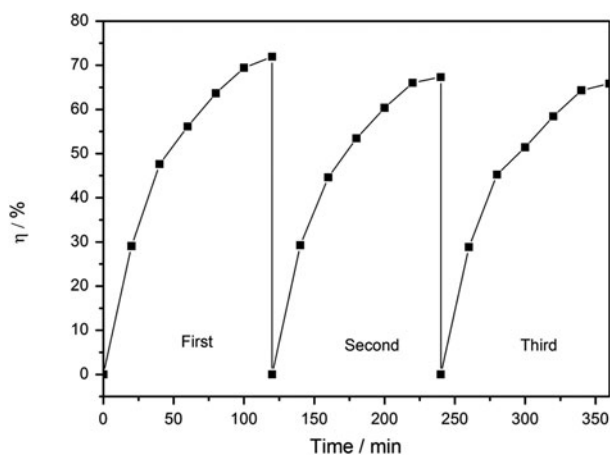


Fig. 9(a). Cycling runs in photocatalytic degradation of reactive brilliant red X-3B.

experiments, the photocatalytic activity of BiOI catalyst decreased slightly. These results also suggest that the catalyst does not decompose or dissolve into aqueous solutions; otherwise, the photocatalytic efficiency would decrease sharply. In addition, from the XRD graphs (Fig. 9(b)) of BiOI before and after the photocatalytic reactions, it was found that the peaks were identical on the whole, indicating that the system was stable. All the results indicated that the photocatalyst kept stable in the photocatalysis.

3.3. Photocatalytic degradation of MO

In order to further study the photocatalytic properties of the as-prepared BiOI catalyst, the degradation

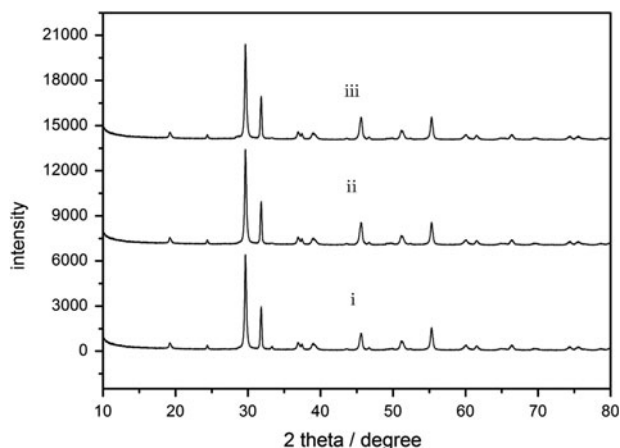


Fig. 9(b). The XRD patterns of BiOI: (i) the fresh sample, (ii) the first cycle, and (iii) the second cycle.

of MO was also investigated under visible light irradiation in this work.

Fig. 10 shows the decrease of the MO concentration under visible light in the presence of BiOI. Both the photolysis of MO under visible light and the adsorption of MO on the BiOI sample in the dark were checked. It can be seen from Fig. 10 that the degradation efficiency of MO is negligible in the absence of catalyst or light irradiation, and the degradation efficiency in the presence of BiOI catalyst is found to be 72.7% after 120-min irradiation. This indicates that MO degradation is mainly attributed to photocatalysis and the photocatalytic activity of BiOI to degrade MO under visible light irradiation is high. In order to evaluate the mineralization degree of MO in water, TOC was monitored before and after the reactions. It is found that about 64.7% of TOC was removed from

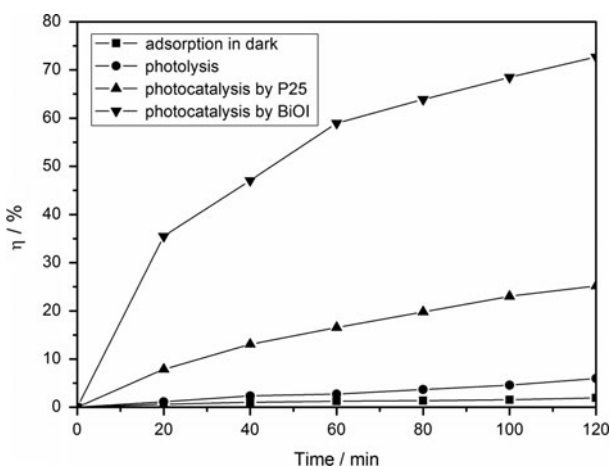


Fig. 10. Photocatalytic efficiency of MO at 10 mg L^{-1} of initial MO concentration, 2.0 g L^{-1} of catalyst dosage, and initial pH 7.

the reaction system (the initial concentration of MO was 10 mg L^{-1} , pH was natural) after 180-min degradation under visible light irradiation, suggesting more than half of MO was mineralized.

4. Conclusions

In the present work, visible light-responding BiOI nanoplates photocatalyst was synthesized, characterized, and used to degrade azo dye wastewater simulated by aqueous reactive brilliant red X-3B solutions under visible light irradiation. The photocatalytic degradation efficiency of MO was also determined under visible light irradiation. It can be concluded that: (1) the synthesis method used in this work is simple, and the chemical property of the catalyst is stable; (2) the catalyst prepared is effective in the decolorization of reactive brilliant red X-3B under visible light irradiation, and the photodegradation efficiency is as high as 95% after 120-min irradiation at mild reaction condition (pH 7, catalyst dosage 2.0 g L^{-1} , reactive brilliant red X-3B concentration 10 mg L^{-1}); (3) The photocatalytic degradation of reactive brilliant red X-3B obeys pseudo-second-order kinetics; (4) the catalyst can be reused for the degradation and its recovery is easy; (5) the BiOI material also exhibits good photocatalytic activity for the degradation of MO under visible light irradiation. It is expected that the BiOI material developed here is a potentially effective photocatalyst for the degradation of reactive dye wastewaters under simulated solar light irradiation.

Acknowledgements

This work was supported financially by the Research Program of Application Foundation and Advanced Technology of Henan Province (Nos. 102300410196 and 122300410177).

References

- [1] N.M. Mahmoodi, M. Arami, H. Bahrami, S. Khorramfar, Novel biosorbent (Canola hull): Surface characterization and dye removal ability at different cationic dye concentrations, *Desalination* 264 (2010) 134–142.
- [2] M. Amini, M. Arami, N.M. Mahmoodi, A. Akbari, Dye removal from colored textile wastewater using acrylic grafted nanomembrane, *Desalination* 267 (2011) 107–113.
- [3] A.R. Tehrani-Bagha, N.M. Mahmoodi, F.M. Menger, Degradation of a persistent organic dye from colored textile wastewater by ozonation, *Desalination* 260 (2010) 34–38.
- [4] A. Maljaei, M. Arami, N.M. Mahmoodi, Decolorization and aromatic ring degradation of colored textile wastewater using indirect electrochemical oxidation method, *Desalination* 249 (2009) 1074–1078.
- [5] H.B. Fu, S.C. Zhang, T.G. Xu, Y.F. Zhu, J.M. Chen, Photocatalytic degradation of RhB by fluorinated Bi_2WO_6 and distributions of the intermediate products, *Environ. Sci. Technol.* 42 (2008) 2085–2091.

- [6] S.B. Zhu, T.G. Xu, H.B. Fu, J.C. Zhao, Y.F. Zhu, Synergetic effect of Bi_2WO_6 photocatalyst with C-60 and enhanced photoactivity under visible irradiation, *Environ. Sci. Technol.* 41 (2007) 6234–6239.
- [7] S.R. Patil, U.G. Akpan, B.H. Hameed, S.K. Samdarshi, A comparative study of the photocatalytic efficiency of Degussa P25, Qualigens, and Hombikat UV-100 in the degradation kinetic of congo red dye, *Desalin. Water Treat.* 46 (2012) 188–195.
- [8] R. Hao, X. Xiao, X.X. Zuo, J.M. Nan, W.D. Zhang, Efficient adsorption and visible-light photocatalytic degradation of tetracycline hydrochloride using mesoporous BiOI microspheres, *J. Hazard. Mater.* 209–210 (2012) 137–145.
- [9] W.D. Wang, F.Q. Huang, X.P. Lin, J.H. Yang, Visible-light-responsive photocatalysts $x\text{BiOBr}-(1-x)\text{BiOI}$, *Catal. Commun.* 9 (2008) 8–12.
- [10] W.D. Wang, F.Q. Huang, X.P. Lin, $x\text{BiOI}-(1-x)\text{BiOCl}$ as efficient visible-light-driven photocatalysts, *Scripta Mater.* 56 (2007) 669–672.
- [11] F. Dong, Y. Sun, M. Fu, W.K. Ho, S.C. Lee, Z. Wu, Novel in situ N-doped $(\text{BiO})_2\text{CO}_3$ hierarchical microspheres self-assembled by nanosheets as efficient and durable visible light driven photocatalyst, *Langmuir* 28 (2012) 766–773.
- [12] F. Dong, Y.J. Sun, W.K. Ho, Z.B. Wu, Controlled synthesis, growth mechanism and highly efficient solar photocatalysis of nitrogen-doped bismuth subcarbonate hierarchical nanosheets architectures, *Dalton Trans.* 41 (2012) 8270–8284.
- [13] F. Dong, S.C. Lee, Z.B. Wu, Y. Huang, M. Fu, W.K. Ho, S.C. Zou, B. Wang, Rose-like monodisperse bismuth subcarbonate hierarchical hollow microspheres: One-pot template-free fabrication and excellent visible light photocatalytic activity and photochemical stability for NO removal in indoor air, *J. Hazard. Mater.* 195 (2011) 346–354.
- [14] F. Dong, W.K. Ho, S.C. Lee, Z.B. Wu, M. Fu, S.C. Zou, Y. Huang, Template-free fabrication and growth mechanism of uniform $(\text{BiO})_2\text{CO}_3$ hierarchical hollow microspheres with outstanding photocatalytic activities under both UV and visible light irradiation, *J. Mater. Chem.* 21 (2011) 12428–12436.
- [15] X.F. Chang, J. Huang, Q.Y. Tan, M. Wang, G.B. Ji, S.B. Deng, G. Yu, Photocatalytic degradation of PCP-Na over BiOI nanosheets under simulated sunlight irradiation, *Catal. Commun.* 10 (2009) 1957–1961.
- [16] F. Dong, Y.J. Sun, M. Fu, Z.B. Wu, S.C. Lee, Room temperature synthesis and highly enhanced visible light photocatalytic activity of porous BiOI/BiOCl composites nanoplates microflowers, *J. Hazard. Mater.* 219–220 (2012) 26–34.
- [17] W.L. Huang, Q.S. Zhu, Structural and electronic properties of BiOX ($X = \text{F}, \text{Cl}, \text{Br}, \text{I}$) considering Bi 5f states, *Comp. Mater. Sci.* 46 (2009) 1076–1084.
- [18] X. Zhang, Z.H. Ai, F.L. Jia, L.Z. Zhang, Generalized one-pot synthesis, characterization, and photocatalytic activity of hierarchical BiOX ($X = \text{Cl}, \text{Br}, \text{I}$) nanoplate microspheres, *J. Phys. Chem. C* 112 (2008) 747–753.
- [19] X.Y. Hu, J. Fan, K.L. Zhang, J.J. Wang, Photocatalytic removal of organic pollutants in aqueous solution by $\text{Bi}_4\text{Nb}_x\text{Ta}_{(1-x)}\text{O}_8\text{I}$, *Chemosphere* 87 (2012) 1155–1160.